

# Three Paleoproterozoic A-type granite intrusions and associated dykes from Kainuu, East Finland



PERTTU MIKKOLA<sup>1)\*</sup>, ASKO KONTINEN<sup>1)</sup>, HANNU HUHMA<sup>2)</sup>,  
YANN LAHAYE<sup>2)</sup>

1) *Geological Survey of Finland, P.O. Box 1237, 70211 Kuopio, Finland*

2) *Geological Survey of Finland, P.O. Box 96, 02151 Espoo, Finland*

## Abstract

Mafic and felsic intrusive rocks aged 2.5–2.4 Ga have been observed over a large area in eastern and northern Finland, as well as in adjacent northwestern Russia. We describe three granite intrusions and associated dykes from Kainuu, Finland, that belong to this bimodal magmatic event. All these three granites show clear A<sub>2</sub>-type chemical affinities with high Y/Nb, HREE, Fe/Mg, Ga and Nb. Two of the intrusions, Rasinkylä and Pussisvaara, were dated at 2425±3 and 2427±3 Ma, respectively, using thermal ionisation mass spectrometry utilizing the chemical abrasion method (CA-TIMS). CA-TIMS ages are supported by single-grain age determinations obtained by using Laser Ablation Multicollector Inductively Coupled Plasma Mass Spectrometer (LA-MC-ICPMS). New data on the previously described Rasimäki granite from southern Kainuu is presented, including an age of 2389±5 Ma obtained with LA-MC-ICPMS. The variable magnetite content of the granites is proposed to reflect the differences in the oxidation state of the source, which in our interpretation is the local Archean lower crust. Partial melting and the emplacement of the granites occurred in an extensional environment. Heat for the partial melting was provided by mafic magmas under and intraplating the extended crust.

**Keywords:** A-type granites, geochemistry, absolute age, isotopes, U/Pb, Paleoproterozoic, Kainuu, Finland

\* Corresponding author email: [perttu.mikkola@gtk.fi](mailto:perttu.mikkola@gtk.fi)

Editorial handling: Joonas Virtasalo

## 1. Introduction

The A-type granitoids have a geochemical signature (high Nb, Ga, Fe/Mg, HREE) that allows them to be distinguished on compositional grounds relatively easily from the other granitoid types (M, S

and I) (Pearce et al., 1984; Whalen et al., 1987; Dall’Agnol & Oliveira, 2007). The A-type granitoids can be subdivided in two major ways: based on the interpreted source, mantle or pre-existing

crust (Eby, 1992), or the oxidation state of the magma, often interpreted as reflecting the characteristics of the source (Dall'Agnol & Oliveira, 2007). One interesting example of A-type granitoid magmatism is the suite of 2.45–2.4 Ga felsic intrusive rocks in eastern Finland (Luukkonen, 1988; Lauri & Mänttari, 2002) and adjacent northwestern Russia (Lobach-Zhuchenko et al., 1998). These granites intruded the Archean craton coevally with voluminous mafic layered intrusions (Alapieti, 1982; Melezhik & Sturt, 1994; Lobach-Zhuchenko et al., 1998; Iljina & Hanski, 2005) and small carbonatites (Lokhov et al., 2009).

In this paper, we present petrographical and geochemical characterization together with zircon U-Pb data for three A-type Paleoproterozoic granite intrusions and associated porphyric dykes from Kainuu, East Finland. We show that the Rasinkylä, Ryysyranta and Pussisvaara granites together with the associated porphyric dykes are ca. 2.43 Ga old and A<sub>2</sub>-type (Eby, 1992) in character. We also present additional data and a new and more precise age determination for the Rasimäki granite dated originally by Vaasjoki et al. (1999). Differences and similarities among these plutons and dykes, as well as A-type intrusions of similar age described earlier from the Western Kareljan Province, will be discussed.

## 2. Geological setting

The Pussisvaara, Ryysyranta and Rasinkylä granite intrusions and associated quartz-feldspar porphyry dykes are located in the Archean Kianta Complex of the Western Kareljan Province in the Fennoscandian Shield (Fig. 1). The surrounding Archean bedrock consists of TTG-gneisses, sanukitoids, paragneisses, leucogranites, amphibolites and diverse migmatites of broadly tonalite-granodiorite cross composition. Proterozoic dolerite dykes are also abundant in the area (Mikkola, 2008).

The Kianta Complex is a classical granite-greenstone terrain discussed in numerous studies during the last decades (e.g. Martin, 1985; Luukkonen, 1992; Vaasjoki et al., 1999; Käpyaho, 2007; Papunen et al., 2009). The Tipasjärvi-Kuhmo-Suo-

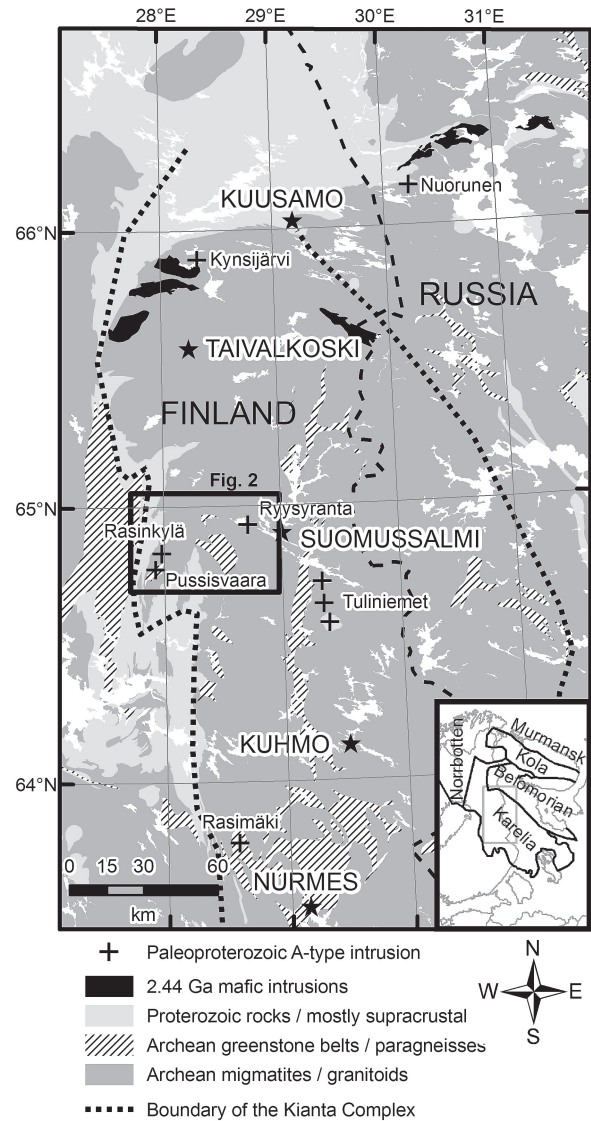


**Fig. 1.** Generalised bedrock map showing locations of the 2.44–2.39 Ga mafic and felsic intrusions, including the intrusions studied here and shown in more detail in Fig. 2. Base map modified from Koistinen et al. (2001).

mussalmi greenstone belt is a north trending narrow stripe of dominantly mafic volcanic rocks. Most of the rocks in the greenstone belt have ages close to 2.8 Ga with some older examples (for references, see Papunen et al., 2009). The TTG magmatism in the gneissic parts of the complex has ages from 2.95 to 2.74 Ga, with a peak close to 2.8 Ga (Vaasjoki et al., 1999; Käpyaho et al., 2006; Lauri et al., 2006).

The TTG magmatism was followed in quick succession by sanukitoid (high-Mg granitoid), quartz diorite and anatectic leucogranite magmatism close to 2.7 Ga (Luukkonen, 1988; Käpyaho et al., 2006; Lauri et al., 2006).

The beginning of the Paleoproterozoic rifting of the Archean nucleus of the Fennoscandian Shield is manifested by mafic intrusions, A-type granitoids and carbonatites, all aged 2.5–2.4 Ga. Large layered mafic intrusions occur over a wide area from northern Finland (Iljina & Hanski, 2005) through Belomorian (Lobach-Zhuchenko et al., 1998) to Kola (Melezhik & Sturt, 1994). A-type granitoids have so far been described from Kuhmo (Luukkonen, 1988: Tuliniemet type), Taivalkoski (Lauri & Mänttari, 2002: Kynsijärvi stock), Oulanka (Lauri et al., 2006: Nuorunen granite) and the Belomorian Belt (Lobach-Zhuchenko et al., 1998). All of these granitoids show typical A-type geochemical features such as high HREE, Fe/Mg, Nb, Zr and Ga. The Rasimäki intrusion further south (Fig. 2) may belong to the same group, but it has not been described in detail chemically or mineralogically. The only published data is the zircon age of  $2352 \pm 25$  Ma, based on extremely discordant analyses (Vaasjoki et al., 1999). The Kynsijärvi quartz alkali feldspar syenite is interpreted as a result of AFC processes between mafic magmas and the Archean crust (Lauri & Mänttari, 2002), while the granites from the Belomorian belt are interpreted as partial melts of the Archean crust heated by mafic magmas (Lobach-Zhuchenko et al., 1998). Recently also carbonatites aged  $2420 \pm 20$  Ma have been described from the Belomorian Belt (Lokhov et al., 2009). Episodic extension of the Archean nucleus of the Fennoscandian Shield over extended time period is indicated by several swarms of dolerite dykes with ages between 2.44 and 1.98 Ga (Vuollo & Huhma, 2005).

The Paleoproterozoic Kainuu schist belt, consisting mainly of siliciclastic metasedimentary rocks and dominantly ca. 2.2 Ga dolerite sills in its lower part, overlays the Archean craton to the west of the study area (Laajoki, 2005). Proterozoic metamorphism has affected the Archean rocks of the study area at 1.85–1.80 Ga causing extensive resetting of

the K-Ar ages of hornblende and biotite (Kontinen et al., 1992).

### 3. Sampling and analytical methods

The Rasinkylä and Ryysyranta stocks were mapped and sampled during the regional bedrock mapping of the Northeast Kainuu area by Geological Survey of Finland (GTK) (Mikkola, 2008). Pussisvaara stock and its surroundings were mapped during an earlier 1:100 000 bedrock mapping program of GTK (Kontinen, 1989).

#### 3.1 Geochemical methods

All analyses were done in the accredited geochemical laboratory of GTK (now Labtium Ltd) in Espoo. Whole rock samples (0.5–1 kg) were crushed with manganese-steel jaw crusher and pulverised in a carbon steel bowl. Pressed pellets were analysed with the X-ray fluorescence method (XRF) for the major elements (Si, Ti, Al, Fe, Mn, Mg, Ca, Na, K, P) and the following trace elements: Ba, Cl, Cr, Cu, Ga, Mo, Ni, Pb, S, Sr and Zn. The inductively coupled plasma mass spectrometer method (ICP-MS) was used for the rest of the analysed trace elements: Ce, Co, Dy, Er, Eu, Gd, Hf, Ho, La, Lu, Nb, Nd, Pr, Rb, Sc, Sm, Ta, Tb, Th, Tm, U, V, Y, Yb and Zr. Total carbon was analysed with the carbon analyser. For detailed descriptions of the applied methods, see Rasilainen et al. (2007).

#### 3.2 Isotope methods

##### 3.2.1 Thermal ionisation mass spectrometer (TIMS)

Representative samples weighing approximately 20 kg were taken from the Rasinkylä and Pussisvaara granites for U-Pb zircon age determination by conventional thermal ionisation mass spectrometer (TIMS). Whole rock Sm-Nd isotope compositions were also determined from the same samples. Analytical procedures follow those described by

Käpyaho et al. (2006). In addition to the air abrasion, the chemical abrasion (CA-TIMS) method (Mattinson, 2005) was used. When applying the CA-TIMS technique, we largely followed the steps described by Schoene et al. (2006), in which zircon grains are placed in beakers in a furnace at 900 °C for 60 hours before being transferred to Teflon microcapsules, placed in high pressure vessels, and leached in 29M HF for 12 hours.

### 3.2.2 Laser Ablation Multicollector Inductively Coupled Plasma Mass Spectrometer (LA-MC-ICPMS)

For LA-MC-ICPMS the zircon grains were mounted in epoxy resin, sectioned approximately in half and polished. Back-scattered electron images (BSE) and cathodoluminescence (CL) pictures of the zircons were taken to target the analysis spots. U–Pb dating analyses were performed utilizing the Nu Plasma HR multicollector ICPMS together with a New Wave UP193 Nd:YAG laser microprobe at the Geological Survey of Finland in Espoo. Samples were ablated in He gas (gas flow = 0.2–0.3 l/min) using a low volume teardrop-shaped (<2.5 cm<sup>3</sup>) laser ablation cell (Horstwood et al., 2003). The He aerosol was mixed with Ar (gas flow = 1.2 l/min) in a teflon mixing cell prior to entry into the plasma. The gas mixture was optimized daily for maximum sensitivity.

All analyses were made in static ablation mode. Ablation conditions were: beam diameter: 25 µm, pulse frequency: 10 Hz, beam energy density: 1.4 J/cm<sup>2</sup>. A single U–Pb measurement included 30 s of on-mass background measurement, followed by 60 s of ablation with a stationary beam. Masses 204, 206 and 207 were measured in secondary electron multipliers, and 238 in the extra high mass Faraday collector. The geometry of the collector block does not allow simultaneous measurement of <sup>208</sup>Pb and <sup>232</sup>Th. Ion counts were converted and reported as volts by the Nu Plasma time-resolved analysis software. <sup>235</sup>U was calculated from the signal at mass 238 using a natural <sup>238</sup>U/<sup>235</sup>U=137.88. Mass number 204 was used as a monitor for common <sup>204</sup>Pb.

In an ICPMS analysis, <sup>204</sup>Hg originates mainly from the He supply. The observed background counting-rate on mass 204 was ca. 1200 (ca. 1.3 × 10<sup>-5</sup> V), and had been stable at that level during the year prior to the measurements. The contribution of <sup>204</sup>Hg from the plasma was eliminated by on-mass background measurement prior to each analysis. Age related common lead (Stacey & Kramers, 1975) correction was used if the analysis showed common lead contents above the detection limit. Signal strengths on mass 206 were typically >10<sup>-3</sup> V, depending on the uranium content and age of the zircon. Two calibration standards were run in duplicate at the beginning and end of each analytical session, and at regular intervals during sessions.

Raw data were corrected for background, laser induced elemental fractionation, mass discrimination and drift in ion counter gains and reduced to U–Pb isotope ratios by calibration to concordant reference zircons of known age, using protocols adapted from Andersen et al. (2004) and Jackson et al. (2004). Standard zircons GJ-01 (609±1 Ma; Belousova et al., 2006) and an in-house standard A1772 (2711±3 Ma/TIMS; 2712±1 Ma/SIMS) were used for calibration. The calculations were done off-line, using an interactive spreadsheet program written in Microsoft Excel/ VBA by T. Andersen (Rosa et al., 2009). To minimize the effects of laser-induced elemental fractionation, the depth-to-diameter ratio of the ablation pit was kept low, and isotopically homogeneous segments of the time-resolved traces were calibrated against the corresponding time interval for each mass in the reference zircon. To compensate for drift in instrument sensitivity and Faraday vs. electron multiplier gain during an analytical session, a correlation of signal vs. time was assumed for the reference zircons. A description of the algorithms used is provided in Rosa et al (2009). Plotting of the U–Pb isotopic data and age calculations were performed using the Isoplot/Ex 3 program (Ludwig, 2003). All the ages were calculated with 2σ errors and without decay constants errors.

## 4. Results

### 4.1 Field observations and petrography

Distinction of the presently studied granites from the hosting granitic Archean bedrock is straightforward both in the field and under the microscope as the former are typically less deformed, mostly clearly porphyritic and practically free of enclaves of any sort. The stocks and the related porphyry dykes lack the banded segregation foliation and the ca. 2.7 Ga migmatization characterising the Archean country rocks, but show apparent schistosity and are cut by faults. Metamorphosed and foliated, probably Paleoproterozoic (Vuollo & Huhma, 2005: 2.44–1.98 Ga), dolerite dykes have been observed to cross-cut the Pussisvaara granite. These field relations sug-

gest that the studied granites intruded between 2.7 Ga and 1.98 Ga.

#### 4.1.1 Rasinkylä granite

The Rasinkylä granite (Fig. 2) has been shortly described by Enkovaara et al. (1953) who considered it as a variety of the Neoproterozoic leucogranites typical for the surrounding area. The granite body is elongated in the northeast direction and is approximately 5 km long and 2 km wide. The western margin of the intrusion is cut by the northeast trending, sinistral Louhijärvi fault. The exact dimensions of the intrusion are difficult to estimate as the contacts are unexposed and as it is geophysically indistinct of the surrounding Archean rocks. Airborne radiation maps provide some hints of the dimensions, but the extensive and variably thick quaternary cover blurs the picture.

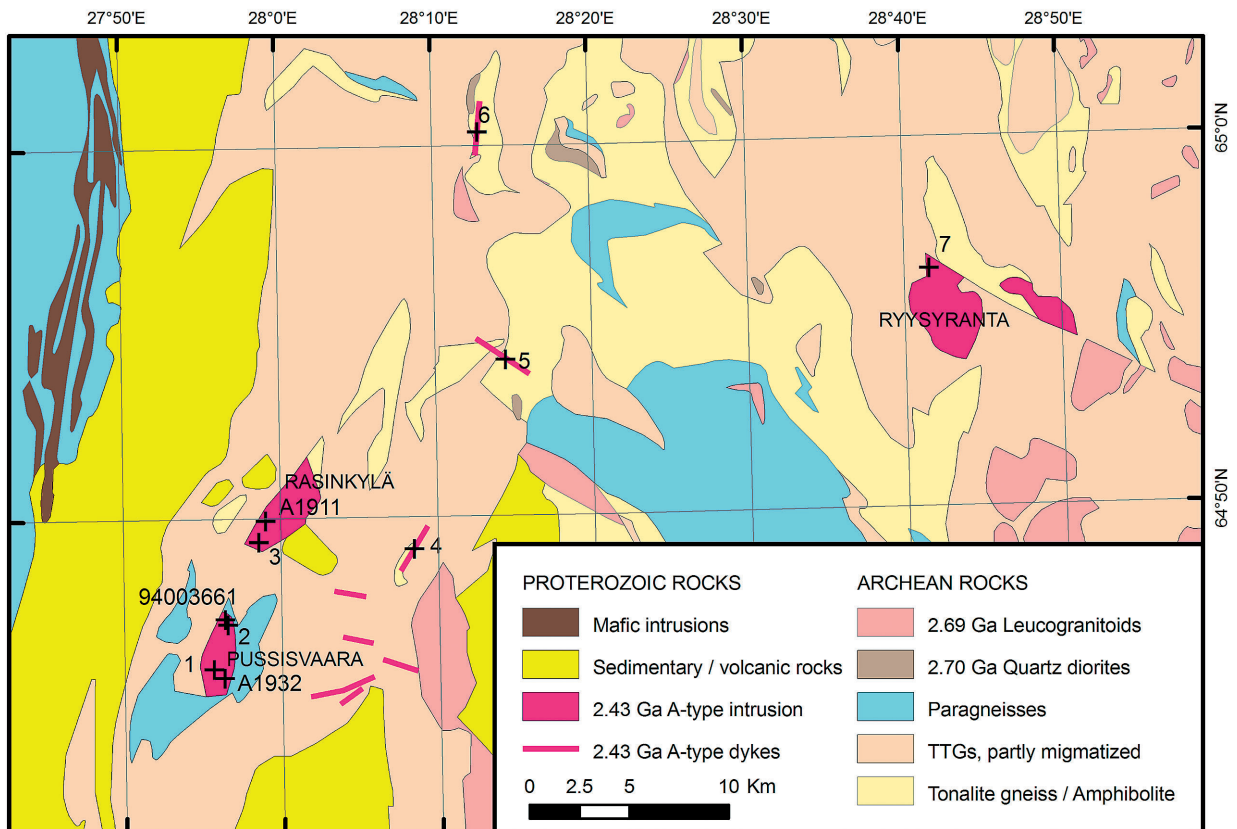


Fig. 2. Geological map of the study area. Based on maps of Kontinen (1989) and Mikkola (2008). Numbers refer to samples listed in Table 1.

The red granite has a slightly foliated microstructure, in which potassium feldspar phenocrysts 0.5–2 cm across are found in a finer grained (1–2 mm) granoblastic groundmass of quartz, potassium feldspar and plagioclase. Accessory minerals include muscovite, biotite, fluorite, chlorite, zircon, apatite and allanite. Muscovite and chlorite are retrogressive, replacing plagioclase and biotite, respectively. Enkovaara et al. (1953) report that the granite locally also contains hornblende, which we however did not observe during the fieldwork or in the thin sections studied.

### 4.1.2 Pussisvaara granite

The Pussisvaara intrusion, elongated in north-south direction, is ca. 4.5 km long and 1.7 km wide (Kontinen, 1989). In contrast to the Rasinkylä granite, the Pussisvaara granite is clearly magnetic allowing interpretation of its size and shape from aeromagnetic maps.

The Pussisvaara granite resembles the Rasinkylä granite in terms of its structural features and mineralogy. However, it shows a more strained microstructure, is generally somewhat richer in biotite and typically contains some magnetite. The magnetite dissemination is weak and variable, but still abundant enough (Table 1) to make the intrusion clearly visible on aeromagnetic maps.

### 4.1.3 Ryysyranta granite

The Ryysyranta intrusion is mostly covered by quaternary deposits. The known outcrops concentrate in a small area just south of the Haukiperä fault. However, the intrusion is magnetic and both its size and shape have been interpreted from aeromagnetic maps. The outcrop and magnetic data suggest that the intrusion was cut into two parts by the southeast trending, dextral Haukiperä fault. Prior to faulting the intrusion seems to have been almost circular and ca. 4 km across.

On the known outcrops the red-coloured Ryysyranta granite has a sheared microstructure. Main mineral constituents are potassium feldspar, quartz and plagioclase, which occur as phenocrysts 1–4 mm

across in a fine-grained (0.1 mm) groundmass consisting of the same minerals plus some biotite and magnetite. In addition, there is minor muscovite and epidote replacing plagioclase.

### 4.1.4 Quartz-feldspar porphyry dykes

Apparently cogenetic quartz-feldspar porphyry dykes occur in the Archean bedrock around the intrusions. These dykes are typically 10–20 meters wide and vary from crosscutting to conformal with respect to the foliations of the surrounding Archean gneisses.

The porphyry dykes vary from red to reddish grey in colour and have a strongly porphyritic character. The phenocrysts scattered in fine-grained (<0.1 mm) granitic groundmass are typically 0.5–1 cm across and comprise resorbed quartz and subhedral feldspars, both plagioclase and potassium feldspar. There is no evidence for glassy or microcrystalline domains in the groundmass or phenocrysts.

## 4.2 Whole-rock geochemistry

Silica versus several major and trace element plots of the granites are shown, together with some reference data, in Figure 3. Most samples are rich in SiO<sub>2</sub> (69.5–78 %) and slightly peraluminous (Table 1: A/CNK=0.96–1.13). Ferromagnesian components are low (Fe<sub>2</sub>O<sub>3</sub>tot=0.97–3.56 %, MgO=0.05–0.93 %) and alkalis high (K<sub>2</sub>O=2.52–6.37 %, Na<sub>2</sub>O=2.71–4.14 %). The Pussisvaara granite is richer in ferromagnesian elements, CaO and P<sub>2</sub>O<sub>5</sub>, than the other granites (Fig. 3; Table 1). All samples have similar and relatively high HREE concentrations and display negative Eu anomalies (Fig. 4). Pussisvaara deviates slightly by showing stronger LREE enrichment (La<sub>N</sub>=335–563 vs. 57–204), more fractionated REE pattern ((La/Yb)<sub>N</sub>=20–42 vs. 1–8) and weaker Eu anomaly (Eu/Eu\*=0.32–0.50 vs. 0.03–0.26). Differences in trace elements are not limited to REEs, as the Pussisvaara granite has also higher Ba (651–1654 vs. 69–467 ppm), Co (2.22–9.9 vs. 0.85–1.81 ppm), Sc (3.91–9.4 vs. <2.77

**Table 1.** Geochemical results of whole rock samples from the Rasinkylä, Ryysyranta, Pussisvaara, Rasimäki granites and porphyry dykes. Susceptibility measurements were made at GTK petrophysical laboratory in Kuopio.

Sample Intrusion	1 Pussisvaara	2 Pussisvaara	A1932 Pussisvaara	94003661* Pussisvaara	3 Rasinkylä	A1911 Rasinkylä	4** Dyke	5 Dyke	6** Dyke	7 Ryysyranta	ATK-2007-1 Rasimäki	94003567** Rasimäki
SiO <sub>2</sub> %	73.40	73.10	75.40	69.50	72.70	76.30	76.60	78.00	77.40	77.10	73.7	74.80
TiO <sub>2</sub>	0.40	0.54	0.29	0.49	0.11	0.08	0.03	0.11	0.11	0.11	0.248	0.11
Al <sub>2</sub> O <sub>3</sub>	13.10	13.10	12.50	14.60	14.90	12.70	13.10	12.00	12.10	12.20	13.30	13.40
Fe <sub>2</sub> O <sub>3</sub> (tot)	2.82	2.88	2.05	3.56	1.42	1.29	0.97	1.31	1.39	1.32	2.33	1.72
MnO	0.04	0.04	0.03	0.06	0.02	0.02	0.02	0.01	0.02	0.02	0.04	0.02
MgO	0.45	0.93	0.36	0.72	0.07	0.05	0.07	0.14	0.07	0.28	0.18	0.18
CaO	1.21	2.23	0.62	1.30	0.43	0.74	0.51	0.16	0.22	0.48	0.88	0.49
Na <sub>2</sub> O	3.05	4.14	2.71	3.38	3.57	3.52	4.13	3.05	3.26	3.29	3.98	3.98
K <sub>2</sub> O	5.10	2.52	5.64	5.85	6.37	4.93	4.22	4.90	5.12	4.81	4.90	5.02
P <sub>2</sub> O <sub>5</sub>	0.11	0.16	0.05	0.15	0.02	b.d.l.	b.d.l.	0.01	b.d.l.	b.d.l.	0.042	b.d.l.
Total	99.68	99.64	99.64	99.61	99.61	99.63	99.65	99.70	99.69	99.61	99.60	99.72
A/CNK	1.03	0.96	1.07	1.02	1.10	1.02	1.07	1.13	1.07	1.06	0.99	1.04
Mg#	24.2	39.0	26.0	28.6	9.3	7.6	12.2	17.9	9.4	29.9	13.5	17.2
Ba ppm	982	651	1063	1654	467	120	69	297	97	325	437	141
C	n.a.	n.a.	n.a.	b.d.l.	105	143	n.a.	185	361	b.d.l.	156	b.d.l.
Cl	92	89	105	140	108	68	b.d.l.	94	71	62	85	80
Co	3.65	9.03	2.22	9.9	1.27	0.90	0.85	0.88	1.01	1.81	1.71	b.d.l.
Cr	b.d.l.	b.d.l.	b.d.l.	b.d.l.	b.d.l.	b.d.l.	b.d.l.	b.d.l.	b.d.l.	b.d.l.	b.d.l.	b.d.l.
Cu	b.d.l.	b.d.l.	b.d.l.	b.d.l.	b.d.l.	b.d.l.	b.d.l.	b.d.l.	b.d.l.	b.d.l.	b.d.l.	b.d.l.
Ga	b.d.l.	b.d.l.	21	24	27	26	31	26	24	24	29	28
Hf	8.92	10.80	7.51	12.5	5.18	5.38	6.44	7.72	8.11	6.76	9.78	7.33
Mo	b.d.l.	b.d.l.	b.d.l.	b.d.l.	b.d.l.	b.d.l.	b.d.l.	b.d.l.	10	b.d.l.	15	b.d.l.
Nb	12.7	12.3	7.4	14.2	19.4	26.7	47.9	22.7	22.6	27.3	26.7	41.4
Ni	b.d.l.	b.d.l.	b.d.l.	b.d.l.	b.d.l.	b.d.l.	b.d.l.	b.d.l.	b.d.l.	b.d.l.	b.d.l.	b.d.l.
Pb	43	b.d.l.	38	28	35	43	53	b.d.l.	b.d.l.	b.d.l.	31	44
Rb	147	60	110	96.3	308	285	395	212	224	144	177	208
S	b.d.l.	b.d.l.	b.d.l.	100	b.d.l.	b.d.l.	b.d.l.	b.d.l.	b.d.l.	b.d.l.	b.d.l.	b.d.l.
Sc	4.17	7.05	3.91	9.4	b.d.l.	0.87	1.30	1.08	2.77	1.52	3.05	b.d.l.
Sr	130	239	99	169	50	30	18	43	29	86	76	40
Ta	0.86	0.71	0.35	0.81	1.71	1.65	4.72	1.26	1.74	1.74	1.64	2.40
Th	22.8	16.3	16.9	26.4	40.2	43.1	44.7	34.2	38.9	31.5	39.2	35.8
U	1.84	1.45	1.13	1.99	5.49	8.05	12.00	3.29	4.34	3.71	4.86	5.89
V	22.5	46.8	10.7	28.0	1.8	1.1	b.d.l.	0.9	b.d.l.	b.d.l.	3.7	13.0
Y	31.9	38.1	18.2	47.0	44.3	49.7	83.6	34.1	38.3	46.1	46.2	52.4
Zn	64	33	48	32	26	31	34	b.d.l.	23	22	64	27
Zr	353	432	299	479	126	107	92	203	200	188	327	191
La	104.0	111.0	116.0	174.0	63.3	29.3	17.8	27.8	53.1	35.2	147.0	53.7
Ce	196.0	203.0	231.0	321.0	106.0	62.2	46.8	76.6	105.0	88.9	303.0	117.0
Pr	19.9	21.1	20.7	34.9	13.3	7.4	6.3	7.7	11.0	9.9	30.2	13.3
Nd	65.5	75.9	65.8	119.0	46.7	27.9	25.4	27.3	34.3	34.8	101.0	44.4
Sm	9.28	10.80	7.98	16.70	8.06	6.27	8.59	5.81	6.90	7.57	13.30	8.39
Eu	1.05	1.68	0.76	1.97	0.63	0.27	0.10	0.22	0.14	0.30	0.88	0.36
Gd	8.30	9.96	6.76	13.90	6.93	6.34	10.20	5.06	5.96	7.25	11.50	7.56
Tb	1.09	1.37	0.88	1.84	1.06	1.17	2.02	0.94	0.99	1.20	1.62	1.19
Dy	5.46	6.99	3.59	8.72	6.38	7.55	14.20	6.00	6.11	7.64	7.86	7.39
Ho	1.11	1.37	0.77	1.73	1.34	1.67	3.05	1.29	1.41	1.68	1.53	1.65
Er	3.34	3.99	1.95	5.24	4.47	5.22	10.50	4.14	4.50	5.46	4.44	5.27
Tm	0.48	0.54	0.28	0.68	0.68	0.88	1.69	0.63	0.77	0.90	0.63	0.83
Yb	3.56	3.78	1.84	4.64	5.15	6.42	12.20	4.73	5.37	6.06	4.43	5.76
Lu	0.51	0.59	0.27	0.64	0.80	0.98	1.76	0.67	0.85	0.88	0.65	0.86
La <sub>N</sub>	335.5	358.1	374.2	561.3	204.2	94.5	57.4	89.7	171.3	113.5	474.2	173.2
(La/Yb) <sub>N</sub>	19.7	19.8	42.5	25.3	8.3	3.1	1.0	4.0	6.7	3.9	22.4	6.3
Eu/Eu*	0.37	0.50	0.32	0.40	0.26	0.13	0.03	0.12	0.07	0.12	0.22	0.14
T zircon (°C)***	859	870	851	882	770	754	746	823	815	808	847	804
TE <sub>173</sub> ****	0.96	0.95	0.97	0.95	0.95	1.02	1.09	1.11	1.01	1.05	1.01	1.01
Susceptibility*****	14060	450	6380	10470	40	30	50	40	70	4660	4500	30

\* From Rasilainen et al. (2007)

\*\* From Mikkola (2008)

\*\*\* after Watson &amp; Harrison (1983)

\*\*\*\* after Irber (1999)

\*\*\*\*\* K(Six10<sup>-6</sup>)

b.d.l. = below detection limit

n.a. = not analysed

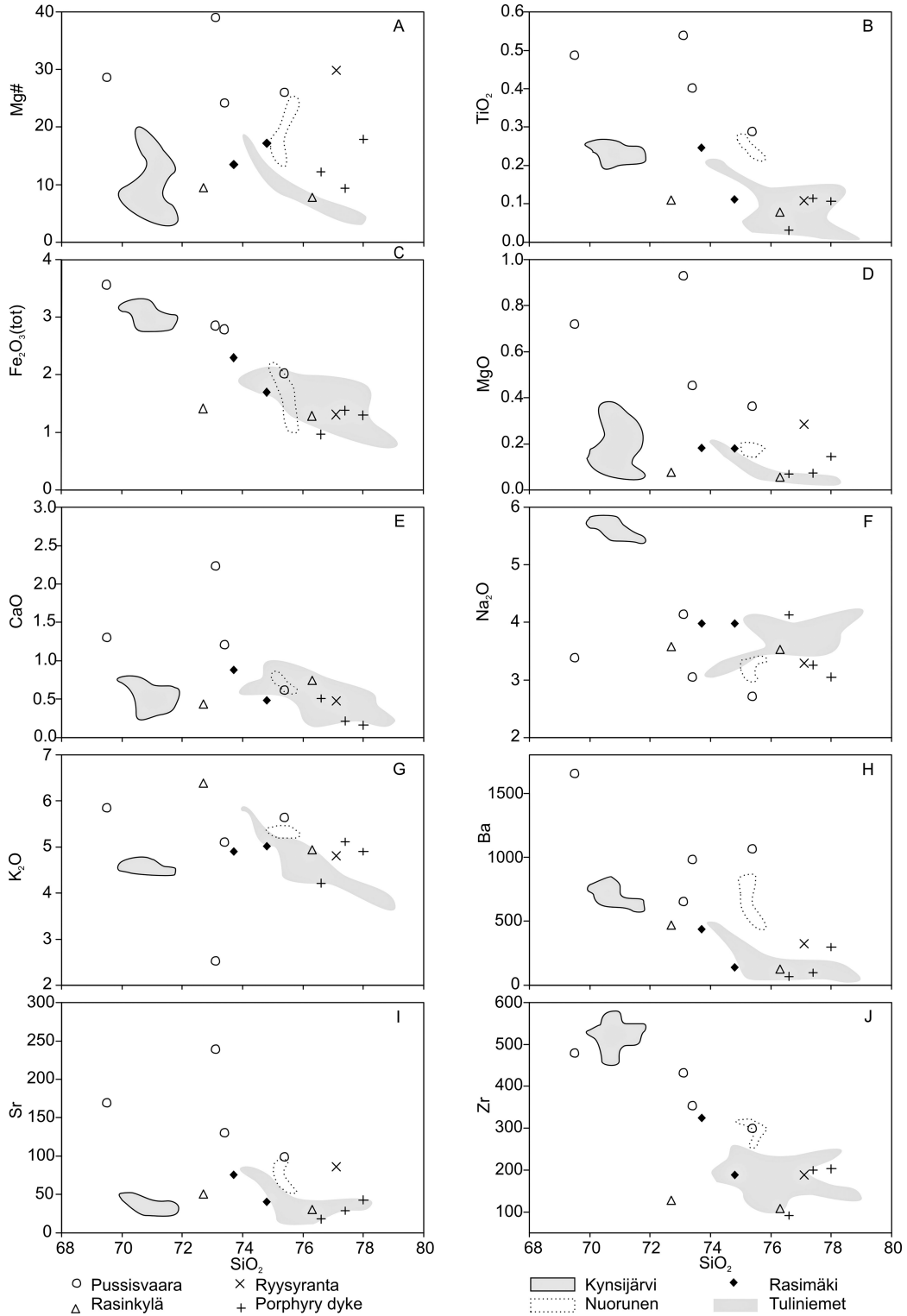


**Fig. 3.** Harker diagrams illustrating geochemical characteristics of the different intrusions. Reference data for Kynsijärvi (Lauri & Mänttari, 2002), Nuorunen (Lauri et al., 2006), Tuliniemet (Rämö & Luukkonen, unpublished data) and Rasimäki (Rasilainen et al., 2007; this study) intrusions are shown. It should be noted that MgO is below detection limit in 8 out of 12 samples from Tuliniemet.

ppm), Sr (99–239 vs. 18–86 ppm), V (10.7–46.8 vs. <1.8 ppm) and Zr (299–479 ppm vs. 92–203 ppm) concentrations. Pussisvaara has lower concentrations in Nb (7.4–14.2 vs. 19.4–47.9 ppm), Rb (60–147 vs. 144–395 ppm), Ta (0.35–0.81 vs. 1.26–4.72 ppm), Th (16.3–26.4 vs. 31.5–44.7 ppm) and U (1.13–1.99 vs. 3.29–12.00 ppm) (Fig. 4). The dyke samples have the most evolved compositions: being the highest in  $\text{SiO}_2$  and lowest in ferromagnesian elements.

In the Y vs. Nb classification diagram of Pearce et al. (1984) the studied granites plot into the field of within-plate granites (WPG) (Fig. 5A), excluding the Pussisvaara intrusion that plots partly in the volcanic arc granite field (VAG). In the classification scheme of Dall’Agnol & Oliveira (2007), all of the samples plot within the field of A-type granites (Fig. 5B). When plotted on Eby’s (1992) diagram for chemical subdivision of A-type granitoids (Fig. 5C), all samples plot within the  $A_2$  field. According to Eby (1992), intrusions plotting in the

$A_2$  field are likely to be derived from recycled crustal sources, while intrusions plotting in  $A_1$  field are probably derived from mantle sources in areas of mantle upwelling.

## 4.3 Isotope results

### 4.3.1 U-Pb Results

Separation of the sample A1911 from the Rasinkylä granite yielded light-coloured, reddish, mostly turbid zircon grains forming simple euhedral prisms. The three analyses made on multigrain fractions show large range in Pb/U, reflecting the intensity of the applied abrasion pretreatment. The unabraded fraction A is extremely discordant (Fig. 6) and contains a large fraction of common lead (Table 2). The fraction B was mechanically abraded for 18 hours and is clearly less discordant. The CA-TIMS fraction C is concordant at  $2427 \pm 3$  Ma. The data from the other multigrain fractions are consistent

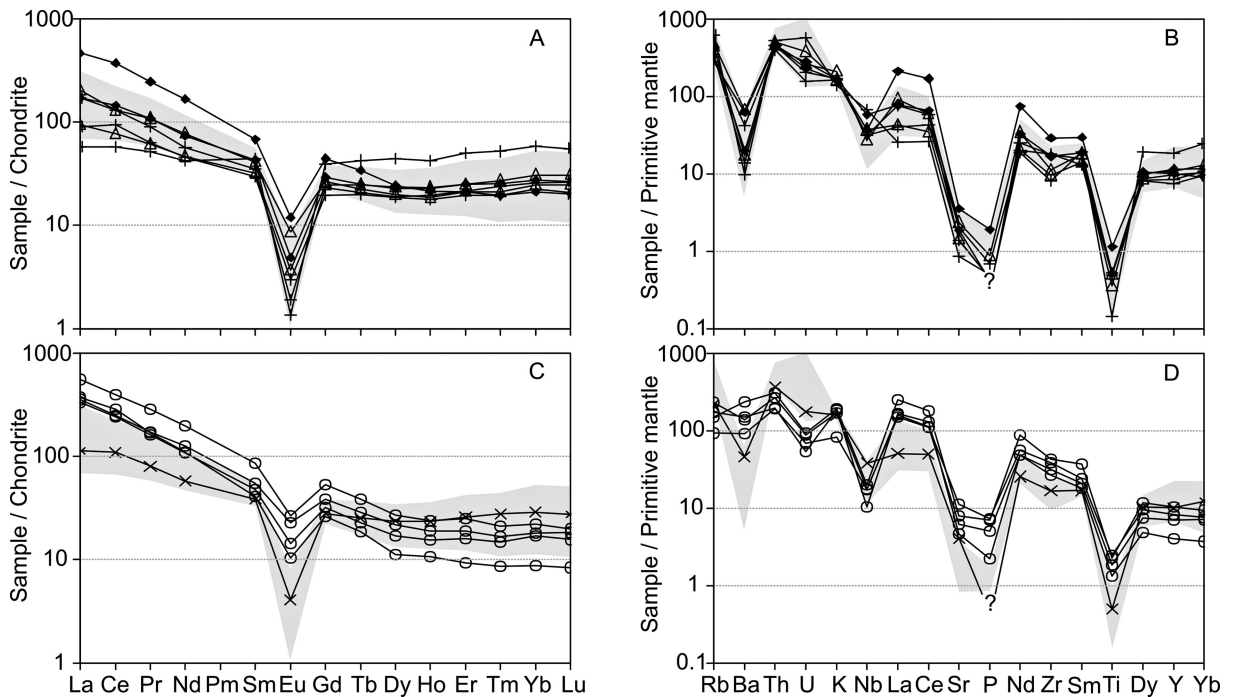


**Fig. 4.** Chondrite-normalised REE and mantle normalised spider diagrams for samples from the Rasinkylä granite (A, B), surrounding granite-porphry dykes (A, B), Rasimäki (A, B), Pussisvaara (C, D) and Ryysyranta (C, D). Symbols as in Figure 3. Shaded field refers to Tuliniemet. Chondrite values from Boynton (1984). Primitive mantle values from Sun & McDonough (1989).

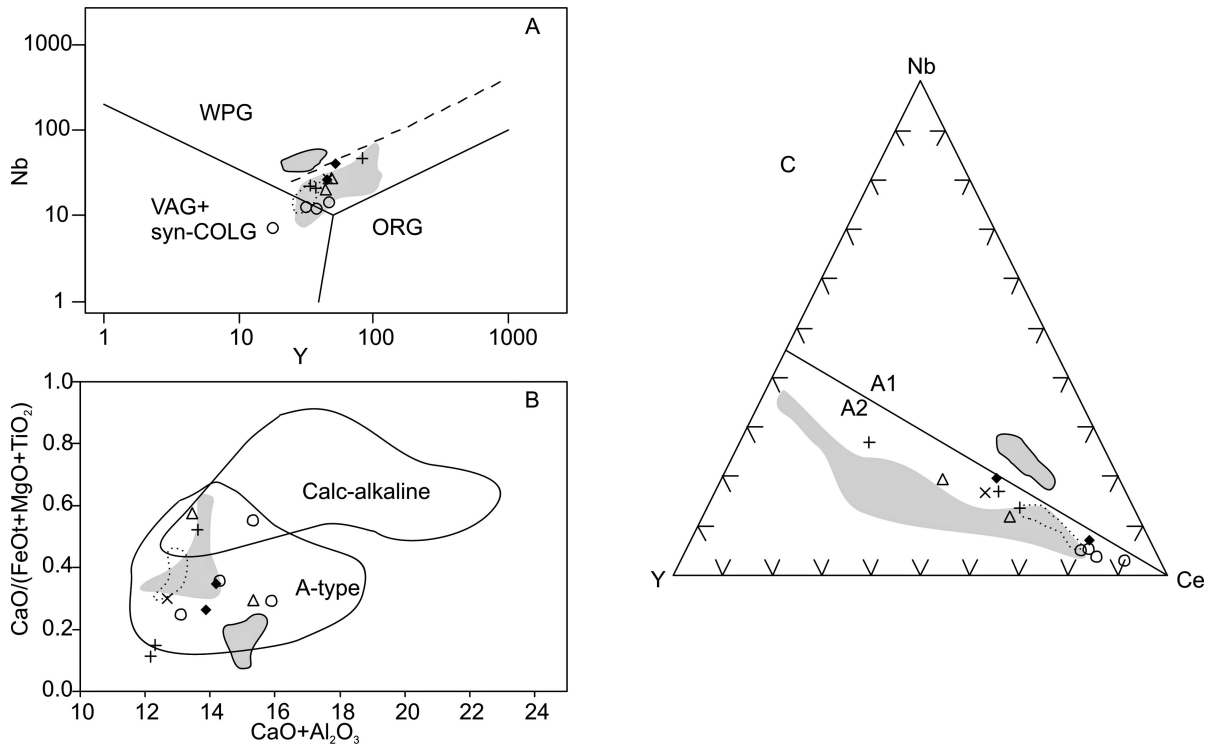


**Fig. 5.** Plots of the studied granites on some classification diagrams for granitoids. (A) Y-Nb diagram of Pearce et al. (1984). WPG=within-plate granites, VAG=volcanic arc granites, syn-COLG=syn-collisional granites, ORG=ocean ridge granites. (B)  $\text{CaO}/(\text{FeO}+\text{MgO}+\text{TiO}_2)$  vs.  $\text{CaO}+\text{Al}_2\text{O}_3$  diagram of Dall'Agnol & Oliveira (2007). (C) Y-Ce-Nb triangle of Eby (1992) for division of A-type granitoids in A<sub>1</sub>- and A<sub>2</sub>- types. Symbols as in Figure 3.

with this age (Fig. 6). From the 20 analyses made with LA-MC-ICPMS, 18 are concordant and define a concordia age of  $2425\pm 6$  Ma (Table 3, Fig. 6B). We consider the concordant CA-TIMS analysis as the best estimate of the age of the Rasinkylä granite.

Sample A1932 from the Pussisvaara granite yielded abundant simple euhedral zircon grains of varying size and clarity. Many of the larger crystals were fairly turbid. The four multigrain analyses made show similar discordia pattern as the analysis for the sample A1911 (Table 2). The unabraded fraction (A) is highly discordant and richest in common lead. The duplicate analyses made on the fraction A (A#1, A#2) provide similar results within the error limits. The mechanically abraded fraction B is less discordant and contains less common lead. The CA-TIMS fraction C is nearly concordant with Pb/Pb age of  $2425\pm 3$  Ma (Figs. 6C, 6D). Out of the 20 spot analyses made with LA-MC-ICPMS,

all but one on a high-U zircon grain are concordant. Additionally one concordant analysis (Table 3: 13a) is ca. 50 Ma older and another ca. 100 Ma younger (Table 3: 9a). The reasons for these anomalous results are not clear. The remaining 17 concordant points define a concordia age of  $2425\pm 6$  Ma (Fig. 6D). This age is consistent with the CA-TIMS data.

The previously published conventional TIMS data on sample A1128 from the Rasimäki granite are slightly heterogeneous and define an upper intercept of  $2352\pm 25$  Ma (Vaasjoki et al 1999; Fig. 6E). These analyses have fairly high amount of common lead and some of the scatter may be due to analytical problems. Nineteen out of the 21 LA-MC-ICPMS analyses made for this study are concordant and define a concordia age of  $2389\pm 5$  Ma, which we interpret as the crystallization age of the Rasimäki granite.

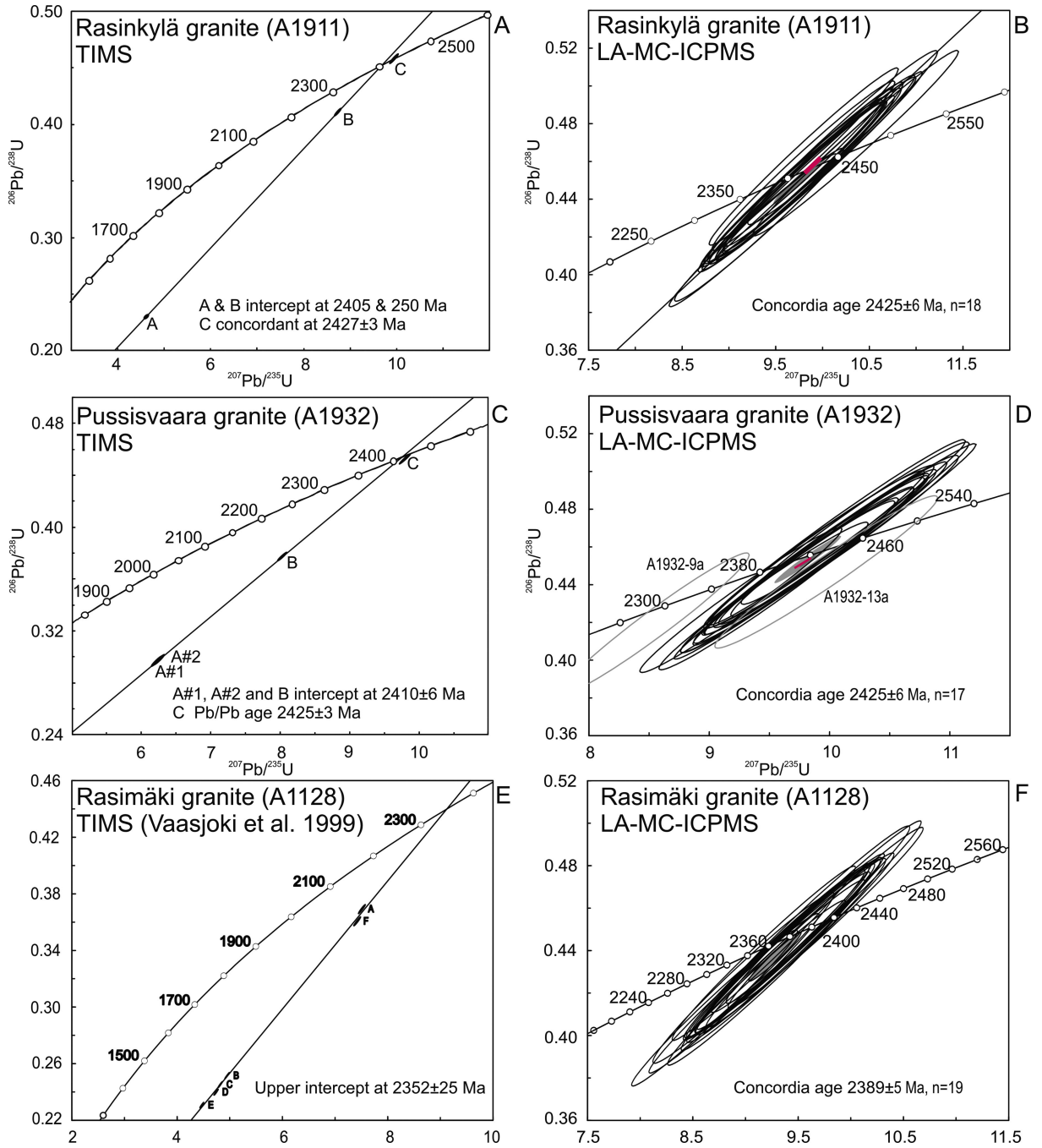


**Fig. 6.** Concordia diagrams for Rasinkylä (A, B), Pussisvaara (C, D) and Rasimäki (E, F) intrusions. Data for E is from Vaasjoki et al. (1999). Error ellipses are drawn at  $2\sigma$ . In figures B, D and F, grey ellipses are the concordia ages calculated from LA-MC-ICPMS analyses and red ellipses are the CA-TIMS analyses.

Table 2. U-Pb data for multigrain zircon fractions analysed with TIMS.

Sample information	Sample weight/ mg	U ppm	Pb ppm	$^{206}\text{Pb}/^{204}\text{Pb}$ measured	$^{208}\text{Pb}/^{206}\text{Pb}$ radiogenic	$^{206}\text{Pb}/^{238}\text{U}$ 2s %	Isotopic ratios* $^{207}\text{Pb}/^{235}\text{U}$ 2s %	$^{207}\text{Pb}/^{206}\text{Pb}$ 2s %	Rho** $^{206}\text{Pb}/^{238}\text{U}$ / $^{207}\text{Pb}/^{235}\text{U}$	Apparent ages / Ma $^{206}\text{Pb}/^{238}\text{U}$ / $^{207}\text{Pb}/^{235}\text{U}$			
<b>A1911 Rasinkylä granite</b>													
(A) p>4.2 g cm <sup>-3</sup> , unabrased	0.38	464	182	158	0.38	0.23018	4.622	0.9	0.14564	0.5	1336	1753	2295
(B) p>4.2 g cm <sup>-3</sup> , >75 µm, abrased 18 h	0.31	209	108	1896	0.27	0.41039	8.728	0.7	0.15425	0.2	2217	2310	2394
(C) p>4.2 g cm <sup>-3</sup> , chemically abrased				4182	0.3	0.45810	9.938	0.7	0.15735	0.15	2431	2429	2427
<b>A1932 Pussivaara granite</b>													
(A#1) p>4.2 g cm <sup>-3</sup> , >75 µm, unabrased	0.57	389	143	1016	0.23	0.29444	6.178	0.7	0.15216	0.2	1664	2001	2370
(A#2) p>4.2 g cm <sup>-3</sup> , >75 µm, unabrased	0.4	357	132	1034	0.23	0.29735	6.232	0.7	0.15199	0.2	1678	2009	2369
(B) p>4.2 g cm <sup>-3</sup> , >75 µm, abrased 17 h	0.46	241	111	3727	0.26	0.37660	8.016	0.7	0.15437	0.2	2060	2233	2395
(C) p>4.2 g cm <sup>-3</sup> , >75 µm, chemically abrased				43560	0.27	0.45235	9.800	0.7	0.15712	0.15	2406	2416	2425

\* Isotopic ratios corrected for fractionation, blank (Pb 10–50 pg) and age related common lead (Stacey &amp; Kramers 1975).

\*\* Error correlation for  $^{207}\text{Pb}/^{235}\text{U}$  vs.  $^{206}\text{Pb}/^{238}\text{U}$  ratios.

Table 3. U-Pb data for spot analysis of zircon grains with LA-MC-ICPMS.

Spot	Measured Ratios				Discordance				Ages									
	U (ppm)	$^{206}\text{Pb}$ (ppm)	$^{206}\text{Pb}/^{204}\text{Pb}$	$^{206}\text{Pb}/^{238}\text{U}$	$^{207}\text{Pb}/^{206}\text{Pb}$	Central (%)	Rho***	$1\sigma$	$^{206}\text{Pb}/^{238}\text{U}$	$1\sigma$	$^{207}\text{Pb}/^{235}\text{U}$	$1\sigma$	$1\sigma$					
<b>A1911 Rasinkylä granite (zircon mounted: ds&lt;4.2 g/cm<sup>3</sup>)</b>																		
A1911-1a	70	54	0.03	9386	0.15635	0.0011	9.746	0.41	0.4521	0.019	0.99	-0.6	2417	12	2411	39	2405	84
A1911-2a	54	44	0.46	2860	0.15988	0.0011	10.354	0.45	0.4697	0.020	0.99	1.4	2454	12	2467	40	2482	88
A1911-3a	75	54	0.06	8469	0.15860	0.0011	9.293	0.38	0.4250	0.017	0.99	-7.7	2441	12	2367	38	2283	78
A1911-4a	33	25	0.00	4644	0.15699	0.0012	9.664	0.41	0.4465	0.018	0.98	-2.2	2423	13	2403	39	2380	82
A1911-5a	158	124	0.37	4058	0.15785	0.0011	9.967	0.42	0.4580	0.019	0.99	-0.1	2433	12	2432	39	2431	84
A1911-6a	34	27	0.00	6422	0.15735	0.0011	9.961	0.42	0.4591	0.019	0.99	0.4	2427	12	2431	39	2436	84
A1911-7a	91	69	0.00	10342	0.15634	0.0011	9.666	0.40	0.4484	0.018	0.99	-1.4	2416	12	2403	38	2388	81
A1911-8a	322	243	0.00	37374	0.15722	0.0011	9.692	0.40	0.4471	0.018	0.99	-2.1	2426	12	2406	38	2382	81
A1911-9a	723	211	4.60	326	0.11988	0.0015	2.909	0.10	0.1760	0.006	0.93	-50.3	1954	23	1384	26	1045	31
A1911-10a	31	24	0.00	9728	0.15364	0.0011	9.799	0.41	0.4626	0.019	0.99	3.2	2387	12	2416	39	2451	85
A1911-11a	68	51	0.00	15578	0.15734	0.0011	9.735	0.39	0.4488	0.018	0.98	-1.8	2427	11	2410	37	2390	79
A1911-12a	857	420	2.50	596	0.14074	0.0013	5.847	0.23	0.3013	0.012	0.97	-27.3	2236	15	1953	34	1698	57
A1911-13a	113	83	0.00	17301	0.15766	0.0011	9.813	0.39	0.4514	0.018	0.99	-1.4	2431	11	2417	37	2402	79
A1911-14a	41	30	0.00	8811	0.15742	0.0011	9.854	0.40	0.4540	0.018	0.98	-0.7	2428	12	2421	38	2413	81
A1911-15a	36	26	0.00	9559	0.15649	0.0011	9.721	0.39	0.4506	0.018	0.98	-1	2418	12	2409	37	2398	79
A1911-16a	37	28	0.00	5000	0.15521	0.0012	9.796	0.40	0.4578	0.018	0.98	1.3	2404	12	2416	38	2430	81
A1911-17a	158	122	0.02	23579	0.15799	0.0010	9.965	0.45	0.4575	0.020	0.99	-0.3	2434	10	2432	42	2428	91
A1911-18a	80	60	0.00	12393	0.15670	0.0011	9.908	0.39	0.4586	0.018	0.98	0.6	2420	11	2426	36	2433	79
A1911-19a	30	23	0.00	17642	0.15675	0.0012	10.215	0.41	0.4727	0.019	0.98	3.7	2421	12	2454	38	2495	82
A1911-20a	110	75	0.17	9024	0.15851	0.0012	9.288	0.36	0.4250	0.016	0.98	-7.6	2440	12	2367	35	2283	72

A1932 Pussisvaara granite (zircon mounted: $d > 4.2 \text{ g/cm}^3$ , +200 mesh)																		
A1932-1a	1852	331	0.00	1662	0.11666	0.0008	1.946	0.06	0.1210	0.004	0.98	-64.8	1906	12	1097	22	736	22
A1932-2a	169	120	0.02	16941	0.15786	0.0011	9.786	0.38	0.4496	0.017	0.98	-1.9	2433	12	2415	35	2393	76
A1932-3a	62	43	0.00	7919	0.15751	0.0011	9.667	0.37	0.4451	0.017	0.98	-2.7	2429	12	2404	35	2373	75
A1932-4a	127	90	0.00	21853	0.15760	0.0011	9.787	0.37	0.4504	0.017	0.98	-1.6	2430	12	2415	35	2397	75
A1932-5a	144	105	0.00	19365	0.15740	0.0011	10.028	0.39	0.4621	0.018	0.98	1	2428	12	2437	36	2449	77
A1932-6a	152	108	0.00	18768	0.15716	0.0011	9.884	0.39	0.4561	0.018	0.98	-0.1	2425	12	2424	36	2422	77
A1932-7a	293	229	0.00	27354	0.15789	0.0011	9.963	0.51	0.4577	0.023	0.99	-0.2	2433	12	2431	48	2429	103
A1932-8a	111	79	0.00	15579	0.15744	0.0011	9.894	0.38	0.4558	0.017	0.98	-0.4	2428	12	2425	35	2421	76
A1932-9a	49	32	0.00	10130	0.14781	0.0013	8.549	0.32	0.4195	0.015	0.97	-3.2	2321	15	2291	34	2258	69
A1932-10a	212	150	0.00	26079	0.15727	0.0011	9.872	0.37	0.4553	0.017	0.98	-0.4	2427	12	2423	35	2419	75
A1932-11a	295	199	0.07	28699	0.15761	0.0011	9.653	0.36	0.4442	0.016	0.98	-3	2430	12	2402	35	2369	73
A1932-12a	74	52	0.02	7948	0.15736	0.0012	9.963	0.38	0.4592	0.017	0.98	0.4	2427	12	2431	35	2436	76
A1932-13a	231	158	0.61	6482	0.16190	0.0014	9.973	0.38	0.4468	0.016	0.97	-4.6	2476	15	2432	35	2381	73
A1932-14a	50	35	0.00	15679	0.15611	0.0012	9.872	0.38	0.4587	0.017	0.98	1	2414	13	2423	35	2434	75
A1932-15a	165	108	0.12	9487	0.15557	0.0011	9.263	0.34	0.4319	0.016	0.98	-4.6	2408	12	2364	34	2314	71
A1932-16a	32	22	0.00	9681	0.15638	0.0012	9.925	0.39	0.4603	0.018	0.98	1.2	2417	13	2428	36	2441	77
A1932-17a	51	36	0.00	6435	0.15767	0.0012	10.127	0.39	0.4659	0.017	0.98	1.7	2431	13	2446	35	2465	77
A1932-18a	152	109	0.00	30166	0.15673	0.0012	10.213	0.39	0.4726	0.018	0.98	3.7	2421	12	2454	35	2495	77
A1932-19a	129	83	0.00	13401	0.15795	0.0012	9.452	0.36	0.4340	0.016	0.98	-5.4	2434	12	2383	35	2324	72
A1932-20a	45	32	0.10	5459	0.15594	0.0012	10.056	0.44	0.4677	0.020	0.99	3.1	2412	12	2440	40	2473	88
A1128 Rasimäki granite (zircon mounted: $d > 4.5 \text{ g/cm}^3$ )																		
A1128-1a	83	61	0.14	7873	0.15290	0.0010	8.706	0.32	0.4130	0.015	0.98	-7.5	2379	11	2308	34	2228	68
A1128-2a	143	107	0.02	24174	0.15357	0.0010	8.891	0.33	0.4199	0.015	0.99	-6.3	2386	10	2327	34	2260	70
A1128-3a	61	48	0.00	11224	0.15353	0.0010	9.272	0.35	0.4380	0.016	0.98	-2.2	2386	11	2365	35	2342	74
A1128-4a	105	82	0.00	15302	0.15165	0.0010	9.174	0.36	0.4387	0.017	0.99	-1	2365	11	2356	35	2345	75
A1128-5a	223	177	0.00	24969	0.15394	0.0010	9.430	0.36	0.4443	0.017	0.99	-1	2390	11	2381	35	2370	75
A1128-6a	151	123	0.00	17061	0.15422	0.0010	9.742	0.38	0.4581	0.018	0.99	1.9	2393	11	2411	36	2431	78
A1128-7a	161	128	0.00	126911	0.15454	0.0010	9.400	0.36	0.4421	0.017	0.99	-1.6	2393	10	2378	35	2360	75
A1128-8a	230	186	0.00	29950	0.15544	0.0010	9.761	0.38	0.4554	0.017	0.99	0.6	2407	10	2412	36	2419	77
A1128-9a	71	56	0.00	6344	0.15517	0.0010	9.518	0.36	0.4449	0.017	0.99	-1.5	2404	11	2389	35	2373	75
A1128-10a	46	36	0.00	5515	0.15474	0.0012	9.428	0.37	0.4419	0.017	0.98	-2	2399	13	2381	36	2359	76
A1128-11a	89	70	0.00	29680	0.15342	0.0010	9.308	0.36	0.4400	0.017	0.99	-1.7	2384	11	2369	36	2351	75
A1128-12a	72	56	0.00	8177	0.15378	0.0010	9.304	0.35	0.4388	0.016	0.98	-2.1	2388	11	2368	35	2345	74
A1128-13a	265	204	0.00	41650	0.15504	0.0010	9.260	0.36	0.4332	0.016	0.99	-4.1	2402	11	2364	35	2320	74
A1128-14a	85	66	0.00	13974	0.15459	0.0011	9.312	0.36	0.4369	0.016	0.98	-3	2397	12	2369	35	2337	74
A1128-15a	97	75	0.00	8493	0.15401	0.0011	9.349	0.36	0.4403	0.017	0.98	-1.9	2391	11	2373	35	2352	74
A1128-16a	56	44	0.00	4555	0.15416	0.0011	9.408	0.36	0.4426	0.017	0.98	-1.5	2393	11	2379	35	2362	75
A1128-17a	40	32	0.00	10219	0.15337	0.0011	9.617	0.39	0.4548	0.018	0.98	1.6	2384	12	2399	37	2416	79
A1128-18a	134	83	0.05	9592	0.15034	0.0010	7.390	0.28	0.3565	0.013	0.98	-18.9	2350	11	2160	33	1966	62
A1128-19a	447	187	1.40	1273	0.14948	0.0011	4.968	0.22	0.2410	0.011	0.99	-44.9	2340	12	1814	38	1392	55
A1128-20a	380	287	0.01	48034	0.15544	0.0010	9.106	0.35	0.4249	0.016	0.98	-6.1	2407	11	2349	35	2282	72
A1128-21a	33	25	0.00	3137	0.15249	0.0011	8.980	0.35	0.4271	0.016	0.98	-4.1	2374	12	2336	36	2293	74

\* Percentage of common  $^{206}\text{Pb}$  in measured  $^{206}\text{Pb}$  calculated from the  $^{204}\text{Pb}$  signal using age-related common lead after model by Stacey & Kramers (1975)

\*\* Errors are absolute  $1\sigma$  values

\*\*\* Error correlation for  $^{207}\text{Pb}/^{235}\text{U}$  vs.  $^{206}\text{Pb}/^{238}\text{U}$  ratios.

Spots highlighted with grey background were omitted from concordia on bases described in the text

### 4.3.2 Sm-Nd results

The Rasinkylä and Pussisvaara samples yield nearly identical initial  $\epsilon_{Nd}$  values (-4.9 and -4.7 respectively), but display clearly differing evolution trends yielding  $t_{DM}$  ages of 3356 and 2889 Ma respectively (Table 4). Both the  $\epsilon_{Nd}$  values at 2.43 Ga and  $t_{DM}$  ages are within the bounds of the variation obser-

ved in the Archean granitoids from the adjacent area (Mikkola & Huhma, unpublished data). The values obtained from the Pussisvaara sample are similar to those from the Kynsijärvi stock (Fig. 7). As the Sm/Nd ratio of the sample from Rasinkylä is relatively high, the older  $t_{DM}$  may reflect fractionation during melt derivation, crystallization or Paleoproterozoic overprinting.

**Table 4.** Whole-rock Sm-Nd isotope data for the age samples.

	Sm (ppm)	Nd (ppm)	$^{147}\text{Sm}/^{144}\text{Nd}$ $\pm 2\sigma$	$^{143}\text{Nd}/^{144}\text{Nd}$ $\pm 2\sigma$	t (Ma)	Initial $\epsilon_{Nd}$	$t_{DM}$ (Ma)
A1911 / Rasinkylä	8.80	36.55	0.1456 $\pm$ 6	0.511572 $\pm$ 10	2427	-4.9	3356
A1932 / Pussisvaara	9.24	63.51	0.0879 $\pm$ 4	0.510664 $\pm$ 10	2425	-4.7	2889

Within run precision for Sm-Nd analysis is  $\pm 2\sigma$  in the last significant digits.  $t_{DM}$  calculated after DePaolo (1981)

## 5. Discussion

The obtained U-Pb zircon ages indicate that the Pussisvaara (2425 $\pm$ 3 Ma) and Rasinkylä (2427 $\pm$ 3 Ma) stocks are of the same age as the Tuliniet intrusions in Kuhmo (Luukkonen, 1988: 2435 $\pm$ 12 Ma). The Kynsijärvi stock ca. 130 km to the north in Taivalkoski is older at 2442 $\pm$ 2 Ma (Lauri & Mänttari, 2002) and the Rasimäki stock ca. 100 km to the south younger at 2389 $\pm$ 5 Ma. Thus, there seems to be a trend to younger emplacement ages from north to south and that the age span of the granite plutonism was at least 40 Ma.

The 2.44–2.39 Ga felsic intrusives form a suite that is distinguishable compositionally, mineralogically and structurally. All these intrusions, excluding Kynsijärvi, are  $A_2$ -type (Fig. 5C) granites suggesting derivation from the local Archean crust. Source heterogeneities could explain the observed compositional scatter, such as highly variable levels of REE fractionation ( $(\text{La}/\text{Yb})_N=1\text{--}42.5$ ) and LREE enrichment ( $\text{La}_N=57\text{--}561$ ) (Table 1; Fig. 4) between the different intrusions. The Sm-Nd isotope data are in line with this interpretation, as the observed initial  $\epsilon_{Nd}$  values are similar to the values of the local Archean basement at 2.43 Ga (Fig. 7). The Kynsi-

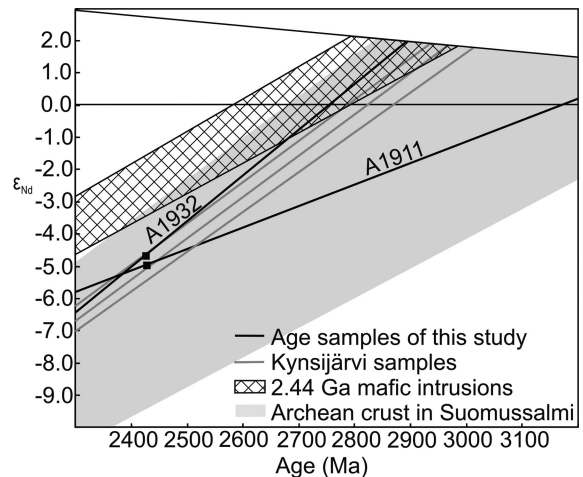


**Fig. 7.**  $\epsilon_{Nd}$  versus age diagram for different rocks and suites. Reference data: Archean crust (Mikkola & Huhma, unpublished data), 2.44 Ga mafic intrusions (Huhma et al., 1990; Hanski et al., 2001), Kynsijärvi (Lauri et al., 2006).

järvi intrusion interpreted as a result of AFC processes (Lauri & Mänttari, 2002) plots on the here applied diagrams (Figs. 3, 5, 6) apart from the other felsic 2.44–2.39 Ga intrusives. It is the only intrusion presenting the  $A_1$ -type indicating mantle derivation (Eby, 1992) (Fig. 5C). Including the granites recognized here, a total of 8 2.44–2.39 Ga  $A$ -

type stocks and numerous related porphyry dykes have been discovered from eastern Finland. Given the extensive Quaternary cover of the area, it is likely that more will be found in the future. For example in the vicinity of Suomussalmi there are several positive magnetic anomalies completely covered by glaciofluvial deposits that may indicate magnetic A-type stocks (Mikkola, 2008). And of course in the case of nonmagnetic intrusions their recognition is even more difficult.

The studied granites are all nearly devoid of wall-rock xenoliths and also of inherited zircons (Fig. 6). Both these features are typical for A-type granitoids often interpreted as products of hot dehydration melting (Frost & Frost, 1997; Dall'Agnol et al., 1999; Dall'Agnol & Oliveira, 2007). Zircon saturation temperatures can be used to estimate the minimum melting temperatures for granites lacking inherited zircons (Miller et al., 2003). Calculated zircon saturation temperatures (Table 1) (Watson & Harrison, 1983) for Pussisvaara vary from 851 to 882 °C, while Rasinkylä and one related dyke yield clearly lower temperatures (746–770 °C). Ryysyranta intrusion and two of the dykes fall between these two estimates (808–823 °C). The results are in the same range as those from the 1.8 Ga A-type Nattanen intrusions in Lapland, for example (Heilimo et al., 2009). The obtained minimum melting temperatures are high enough for dehydration melting of Archean TTGs (Watkins et al., 2007) and for complete zircon dissolution (Miller et al., 2003). In these aspects, this Paleoproterozoic A-type event differs fundamentally from the previous partial melting event in the Kianta Complex that at 2.7 Ga produced granitoids containing abundant inherited zircons (Käpyaho et al., 2006) and enclaves. The maximum melting temperatures calculated for these 2.7 Ga granitoids with zircon saturation thermometry are below 750 °C (based on analysis in Mikkola, 2008).

The observed differences in zircon saturation temperatures can be interpreted in two ways. There could have been a real difference in the local melting temperatures resulting in higher degree of melting and higher zircon content in the Pussisvaara stock, which would also explain the lower Fe/Mg

ratio (Anderson & Morrison, 2005) and the less evolved geochemical nature of the Pussisvaara stock in general (Fig. 3). Alternatively, as the calculated temperatures are minimum ones, it is as well possible that the melting in all cases occurred under similar conditions, but within an heterogeneous source. In the case of Pussisvaara, the source could have been simply richer in Zr. Miller et al. (2003) have calculated that during partial melting of typical crustal rocks, Zr concentration of the melt can be twice as high as that of the source at the point when zircon dissolution temperature is reached. Thus the range in the Zr content of the local TTGs, typically from 100 to 200 ppm (Mikkola, unpublished data), is alone enough to explain the observed differences in zircon concentrations (92–432 ppm) and saturation temperatures, without need for assuming significant differences in melting temperatures for these relatively closely spaced intrusions. However, based on available data it is not possible to eliminate either of the possibilities.

The 2.44–2.39 Ga felsic intrusions may be divided into magnetic (Kynsijärvi, Pussisvaara, Ryysyranta, Rasimäki, Nuorunen) and nonmagnetic (Rasinkylä, Tuliniemet, porphyric dykes) suggesting variably oxidising conditions during crystallisation or later during deformation and metamorphism. This division is to some extent reflected in the plot of the granites on the classification diagram of Dall'Agnol and Oliveira (2007). The magnetic samples plot in or close to the oxidised field and nonmagnetic ones in or close to the reduced field (Fig. 8), excluding the Kynsijärvi samples that plot out of both fields. This division can be explained as a result of variation in the composition and oxidation state of the source (Frost & Frost, 1997; Dall'Agnol et al., 1999; Anderson & Morrison, 2005; Dall'Agnol et al., 2005). It has been suggested that magnetite bearing (oxidised, magnetic) rocks would have their source in oxidised intermediate to felsic igneous rocks (Dall'Agnol et al., 1999; Anderson & Morrison, 2005) and magnetite free (reduced, nonmagnetic) in tholeiitic rocks (Frost & Frost 1997) or in quartz-feldspathic igneous rocks (Anderson & Morrison, 2005), possibly with contribution from sedimentary rocks (Dall'Agnol et al.,

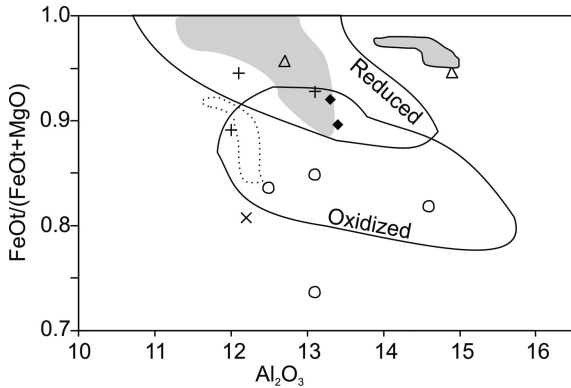


**Fig. 8.** Studied granites on  $\text{Al}_2\text{O}_3$  vs.  $\text{FeOt}/(\text{FeOt}+\text{MgO})$  diagram of Dall'Agnol and Oliveira (2007) designed to separate reduced and oxidised A-type magmas. Symbols as in Figure 3.

2005). All of the mentioned source types are met in the Kianta Complex. It should be noted that Rämö and Luukkonen (2001) report magnetite as an accessory mineral in the Tuliniemet granites. However, magnetite in these granites must be extremely rare and/or sporadically distributed as the intrusions appear nonmagnetic on geophysical maps.

It is worth noting that the Nattanen granite (1.78 Ga) in northern Finland shows fractionation-controlled evolution from oxidised towards reduced compositions, but only the small-volume, late-stage aplitic dykes are nonmagnetic (Heilimo et al., 2009). Our magnetite free dyke samples may have evolved similarly. However, for the nonmagnetic Rasinkylä intrusion, this would require a considerable volume of oxidised granite below the current erosion level, which we consider an unlikely scenario. Furthermore, as Rasinkylä and Pussisvaara have similar  $\text{SiO}_2$  concentrations but clearly differing Mg# and concentrations of, for example, MgO, FeOt,  $\text{TiO}_2$ , Zr, Ba, Sr, U, Th, Ta and Nb (Fig. 3; Table 1), these two magma types can not be realistically linked through fractional crystallization, but would require trace element distribution differing from the normal CHARGE and RADIUS Controlled (CHARAC: Bau, 1996) one. The enrichment in volatiles in the late stages of magmatic evolution can result in non-CHARAC distribution of trace elements through complexation (Bau, 1996). For example, the behaviour of REEs under

such conditions is controlled by the filling state of electron orbit 4f, that splits the REEs into four subsections: La-Nd, Pm-Gd, Gd-Ho and Er-Lu, which tend to show positive anomalies in the REE patterns of rocks evolved in non-CHARAC conditions.

Non-CHARAC behaviour can be recognised visually from REE pattern and from specific plots (Bau, 1996) or it can be estimated mathematically (Irber, 1999). Chondrite normalised REE patterns of our samples have smooth patterns indicating CHARAC conditions, with the possible exception of two dyke samples depleted in LREE (Fig. 4A). In Zr/Hf vs. Y/Ho diagram (Fig. 9), one sample from both Rasinkylä and dykes plot clearly outside the CHARAC field. If the mathematical approach is used, only one sample (5) has a  $\text{TE}_{1,3}$  value (1.11) higher than the Irber's (1999) limit of 1.1 for samples being clearly affected by the tetrad effect. It however plots within the CHARAC field in Figure 9. In contrast, all samples outside the CHARAC field in Figure 9 have  $\text{TE}_{1,3}$  values below 1.1. Consequently, some of the samples might show weak non-CHARAC behaviour, but clearly this is not the root of the observed compositional differences.

Svecofennian heating and deformation processes certainly have affected the intrusions at 1.85–1.80 Ga (Kontinen et al., 1992) and could have caused the breakdown of magnetite in the nonmag-

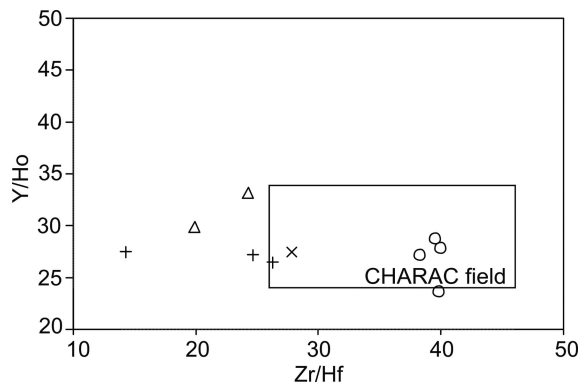


**Fig. 9.** Zr/Hf versus Y/Ho diagram of Bau (1996), where compositions of rocks with chondritic ( $\pm 30\%$ ) Zr/Hf and Y/Ho ratios will plot inside the CHARAC field. Compositions outside the bordered field might indicate non-CHARAC behaviour. Symbols as in Figure 3.

netic intrusions. As the magnetic Pussisvaara and nonmagnetic Rasinkylä intrusions are located just 10 km apart and seem to have experienced roughly similar post-crystallisation deformation and metamorphism, this seems an unlikely scenario. Thus, and based on the discussion above, the observed differences in the magnetic characters of the different intrusions are considered as original magmatic features most likely caused by slightly differing sources. A similar case has been observed for example in the Carajás region in Brazil, where closely spaced 1.9 Ga A-type granitoids also show both oxidised and reduced character (Dall'Agnol et al., 2005). A larger scale example of source-controlled distribution of oxidised and reduced types is provided by the Mesoproterozoic A-type granites of Laurentia and Baltica (Anderson & Morrison, 2005).

It has been previously proposed that the Paleoproterozoic A-type granitoid intrusions of the Karelian Province and the Belomorian Belt are genetically connected to the coeval mafic magmatism (Lobach-Zhuchenko et al., 1998; Rämö & Luukkonen, 2001; Lauri & Mänttari, 2002). There are signs of the coeval mafic magmatism throughout the Kianta Complex (Iljina & Hanski, 2005; Vuollo & Huhma, 2005), but at a much higher volume in Taivalkoski than in Kainuu. In Taivalkoski, large mafic intrusions are observed together with the Kynsijärvi intrusion, and the latter has been interpreted as a product of AFC processes between mafic magmas and the Archean basement (Lauri & Mänttari, 2002). In Kainuu, the mafic intrusions are smaller and the granitoids are partial melts of the Archean basement (Figs. 5C, 7). In both subareas, the heat source was the intra and underplating mafic magmas. An alternative explanation for the partial melting would be thermal relaxation of a thickened crust, but in the Kianta Complex, it occurred already at 2.70–2.67 Ga, shortly after a major Neoproterozoic thickening (Kontinen & Paavola, 2006; Käpyaho, 2007). At 2.5 Ga, the crust was already deeply eroded and there are no signs for re-thickening between 2.65 and 2.45 Ga, which represents a distinct period of quiescence in the metamorphic and magmatic history of the Kianta Complex.

Our new findings add to the growing evidence that the 2.5–2.4 Ga bimodal magmatic event was spatially more extensive than previously thought, possibly shield-wide. Extension and magmatism occurred over a wide area and cannot easily be constrained to a single rift zone, like the modern East African rift, for example. In many ways, the 2.5–2.4 Ga magmatism starts to resemble the classical Mesoproterozoic rapakivi magmatism and associated mafic magmatism in southern Finland (Rämö & Haapala, 2005). Both events occurred ~200 Ma after a major crust-forming event, and in both cases the Sm-Nd systematics of the felsic rocks resemble those of the local older crust. Neither of these extensional events led to a break-up of the crust, but instead both were followed by episodic dolerite dyke magmatism lasting for 500 Ma (Vuollo & Huhma, 2005; Kohonen & Rämö, 2005). The most obvious difference is that for the Paleoproterozoic event the mafic/felsic magma ratio is higher than for the Mesoproterozoic event, at least in the current erosion level. Both events are commonly interpreted as a result of partial melting of mantle and lower crust, but the ultimate reason behind the melting remains poorly constrained. Kukkonen and Lauri (2009) suggested that the trigger for the Mesoproterozoic event might have been the preceding 200 Ma of thermal insulation by the sialic crust which raised the upper mantle and lower crust temperatures high enough to yield melting and trigger the bimodal magmatism. When the similarities of the events preceding and following these two Proterozoic periods of bimodal magmatism are taken into account, it would be worthwhile to test if the model suggested for the younger one is valid for the older one, too.

## 6. Conclusions

The zircon U-Pb ages obtained for the Rasinkylä and Pussisvaara granites and interpreted as crystallisation ages are similar within error limits, being  $2427 \pm 3$  and  $2425 \pm 3$  Ma respectively. The Rasimäki granite yielded an age of  $2389 \pm 5$  Ma and is thus distinctly younger, albeit geochemically indistinguishable from the other stocks.

Rasinkylä, Pussisvaara, Ryysyranta granites and the associated porphyry dykes belong to the suite of felsic 2.44–2.39 Ga A-type intrusions of eastern Finland. Compositional and isotopical evidence suggest their origin through partial melting of heterogeneous Archean lower crust.

The present magnetic character (i.e. magnetite content) of the granites seems to reflect differences in the oxidation state of the source rather than differences in crystallisation and postcrystallisation events.

The new findings add to the expanding evidence of a shield-wide nature of the 2.5–2.4 Ga bimodal magmatic event and its kinship with the Mesoproterozoic bimodal rapakivi events.

## Acknowledgements

Matti Karhunen, Arto Pulkkinen, Tuula Hokkanen and Hugh O'Brien are acknowledged for isotope sample preparation and help with the analyses. This is a SIGL (Finland Isotope Geosciences Laboratory) contribution. Tapani Rämö and Erkki Luukkonen kindly permitted the use of their unpublished data from the Tuliniemet granites as a reference material. Mikko Pitkänen checked the English language. Thorough reviews by Professors Tom Andersen and Roberto Dall'Agnol together with the editorial handling by Joonas Virtasalo improved and clarified the original manuscript significantly. The first author was funded by Academy of Finland during the writing stages of this study (grant number 130066).

## References

- Alapieti, T., 1982. The Koillismaa layered igneous complex, Finland – its structure, mineralogy and geochemistry, with emphasis on the distribution of chromium. *Geological Survey of Finland, Bulletin* 319, 1–116.
- Andersen T, Griffin W.L., Jackson S.E., Knudsen T.-L. & Pearson N.J., 2004. Mid-Proterozoic magmatic arc evolution at the southwest margin of the Baltic Shield. *Lithos* 73, 289–318.
- Anderson, J.L. & Morrison, J., 2005. Ilmenite, magnetite, and peraluminous Mesoproterozoic anorogenic granites of Laurentia and Baltica. *Lithos* 80, 45–60.
- Bau, M., 1996. Controls on the fractionation of isovalent trace elements in magmatic and aqueous systems: evidence from Y/Ho, Zr/Hf, and lanthanide tetrad effect. *Contributions to Mineralogy and Petrology* 123, 323–333.
- Belousova E.A., Griffin W.L. & O'Reilly S.Y., 2006. Zircon crystal morphology, trace element signatures and Hf isotope composition as a tool for petrogenetic modeling: examples from Eastern Australian granitoids. *Journal of Petrology* 47, 329–353.
- Boynnton, W.V., 1984. Cosmochemistry of the rare earth elements: meteorite studies. In: Henderson, P. (ed.). *Rare Earth Element Geochemistry*. Elsevier, Amsterdam, pp. 63–114.
- Dall'Agnol, R. & de Oliveira, D.C., 2007. Oxidized, magnetite-series, rapakivi-type granites of Carajás, Brazil: Implications for classification and petrogenesis of A-type granites. *Lithos* 93, 215–233.
- Dall'Agnol, R., Teixeira, N.P., Rämö, O.T., Moura, C.A.V., Macambira, M.J.B. & de Oliveira, D.C., 2005. Petrogenesis of the Paleoproterozoic rapakivi A-type granites of the Archean Carajás metallogenic province, Brazil. *Lithos* 80, 101–129.
- DePaolo, D.J., 1981. Neodymium isotopes in the Colorado Front Range and crust-mantle evolution in the Proterozoic. *Nature* 291, 684–687.
- Eby, G.N., 1992. Chemical subdivision of the A-type granitoids: Petrogenetic and tectonic implications. *Geology* 20, 641–644.
- Enkovaara, A., Härme, M. & Väyrynen, H., 1953. The General geological map of Finland 1:400 000, explanations to the map of rocks C5-B5 Oulu-Tornio, 153 p. (in Finnish with English summary).
- Frost, C.D. & Frost, B.R., 1997. Reduced rapakivi-type granites: The tholeiite connection. *Geology* 25, 647–650.
- Hanski, E., Walker, R.J., Huhma, H. & Suominen, I., 2001. The Os and Nd isotopic systematics of c. 2.44 Ga Akanvaara and Koitelainen mafic layered intrusions in northern Finland. *Precambrian Research* 109, 73–102.
- Heilimo, E., Halla, J., Lauri, L.S., Rämö, O.T., Huhma, H., Kurhila, M.I. & Front, K., 2009. The Paleoproterozoic Nattanen-type granites in northern Finland and vicinity – a postcollisional oxidized A-type suite. *Bulletin of the Geological Society of Finland* 81, 7–38.
- Horstwood, M.S.A., Foster, G.L., Parrish, R.R., Noble, S.R. & Nowell, G.M., 2003. Common-Pb corrected in situ U–Pb accessory mineral geochronology by LA-MC-ICP-MS. *Journal of Analytical Atomic Spectrometry* 18, 837–846.
- Huhma, H., Cliff, R.A., Perttunen, V. & Sakko, M., 1990. Sm–Nd and Pb isotopic study of mafic rocks associated with early Proterozoic continental rifting: the Peräpohja Schist Belt in northern Finland. *Contributions to Mineralogy and Petrology* 104, 369–379.
- Iljina, M. & Hanski, E., 2005. Layered mafic intrusions of the Tornio-Näränkäväära belt. In: Lehtinen et al. (eds.) *Precambrian Geology of Finland: Key to the Evolution of the Fennoscandian Shield*. Developments in Precambrian Geology 14. Elsevier, Amsterdam, pp. 101–137.
- Irber, W., 1999. The lanthanide tetrad effect and its correlation with K/Rb, Eu/Eu\*, Sr/Eu, Y/Ho, and Zr/Hf of evol-

- ving peraluminous granite suites. *Geochimica et Cosmochimica Acta* 63, 489–508.
- Jackson S.E., Pearson N.J., Griffin W.L. & Belousova E.A., 2004. The application of laser ablation-inductively coupled plasma-mass spectrometry to in-situ U–Pb zircon geochronology. *Chemical Geology* 211, 47–69.
- Käpyaho, A., 2007. Archaean crustal evolution in eastern Finland: new geochronological and geochemical constraints from the Kuhmo terrain and the Nurmes belt. *Geological Survey of Finland*, 20 p.
- Käpyaho, A., Mänttari, I. & Huhma, H., 2006. Growth of Archaean crust in the Kuhmo district, eastern Finland: U–Pb and Sm–Nd isotope constraints on plutonic rocks. *Precambrian Research* 146, 95–119.
- Kohonen, J. & Rämö, O.T., 2005. Sedimentary rocks, diabases, and late cratonic evolution. In: Lehtinen et al. (eds.) *Precambrian Geology of Finland: Key to the Evolution of the Fennoscandian Shield*. *Developments in Precambrian Geology* 14. Elsevier, Amsterdam, pp. 563–603.
- Koistinen, T., Stephens, M.B., Bogatchev, V., Nordgulen, Ø., Wennerström, M. & Korhonen, J., 2001. Geological map of the Fennoscandian Shield, scale 1:2 000 000. *Geological Survey of Finland: Geological Survey of Norway: Geological Survey of Sweden: Ministry of Natural Resources of Russia*.
- Kontinen, A., 1989. Hyrnsalmi. Geological map of Finland 1:100 000, pre-Quaternary rocks, sheet 3443, Geologian tutkimuskeskus.
- Kontinen, A. & Paavola, J., 2006. A preliminary model of the crustal structure of the eastern Finland Archaean complex between Vartiuss and Vieremä, based on constraints from surface geology and FIRE 1 seismic survey. In: *Finnish Reflection Experiment FIRE 2001–2005*. *Geological Survey of Finland, Special Paper* 43, 223–240.
- Kontinen, A., Paavola, J. & Lukkarinen, H., 1992. K–Ar ages of hornblende and biotite from Late Archaean rocks of eastern Finland - interpretation and discussion of tectonic implications. *Geological Survey of Finland, Bulletin* 365, 1–31.
- Kukkonen, I.T. & Lauri, L.S., 2009. Modelling the thermal evolution of a collisional Precambrian orogen: high heat production migmatitic granites of southern Finland. *Precambrian Research*, 233–246.
- Laajoki, K., 2005. Karelian supracrustal rocks. In: Lehtinen et al. (eds.) *Precambrian Geology of Finland: Key to the Evolution of the Fennoscandian Shield*. *Developments in Precambrian Geology* 14. Elsevier, Amsterdam, pp. 279–341.
- Lauri, L.S. & Mänttari, I., 2002. The Kynsijärvi quartz alkali feldspar syenite, Koillismaa, eastern Finland - silicic magmatism associated with 2.44 Ga continental rifting. *Precambrian Research* 119, 121–140.
- Lauri, L.S., Rämö, O.T., Huhma, H., Mänttari, I. & Räsänen, J., 2006. Petrogenesis of silicic magmatism related to the 2.44 Ga rifting of Archean crust in Koillismaa, eastern Finland. *Lithos* 86, 137–166.
- Lobach-Zhuchenko, S.B., Arestova, N.A., Chekulaev, V.P., Levsky, L.K., Bogomolov, E.S. & Krylov, I.N., 1998. Geochemistry and petrology of 2.40–2.45 Ga magmatic rocks in the northwestern Belomorian Belt, Fennoscandian Shield, Russia. *Precambrian Research* 92, 223–250.
- Lokhov, K.I., Sibelev, O.S., Slabunov, A.I., Bogomolov, E.S. & Prilepsky E.B., 2009. Endogenous and sedimentary carbonate rocks from the Belomorian province: new geochemical, isotopic and geochronological data. Abstracts of XXVI International Conference School “Geochemistry of Alkaline Rocks”. Moscow: GEOKHI RAS, 93–94.
- Ludwig, K.R., 2003. *Isoplot/Ex 3. A Geochronological Toolkit for Microsoft Excel*. Berkeley Geochronology Center, Special Publication No. 4.
- Luukkonen, E.J., 1988. Moisiovaara and Ala-Vuokki, Explanation to the geological map of Finland 1:100 000, Pre-Quaternary rocks, sheets 4421, 4423+4441, 90 p. (in Finnish with English summary).
- Luukkonen, E.J., 1992. Late Archaean and early Proterozoic structural evolution in the Kuhmo-Suomussalmi terrain, eastern Finland. *Annales Universitatis Turkuensis, Ser. AII* 78, 1–76.
- Martin, H., 1985. Nature, origine et évolution d’un segment de croûte continentale archéenne : contraintes chimiques et isotopiques. Exemple de la Finlande. *Memoires et Documents du Centre Armoricaïn d’Etude Structurale des Socles* 1, Université de Rennes, 324 p.
- Mattinson, J.M., 2005. Zircon U–Pb chemical abrasion (“CA-TIMS”) method: Combined annealing and multi-step partial dissolution analysis for improved precision and accuracy of zircon ages. *Chemical Geology* 220, 47–66.
- Melezhik, V.A. & Sturt, B.A., 1994. General geology and evolutionary history of the early Proterozoic Polmak-Pasvik-Pechenga-Imandra/Varzuga-Ust’Ponoy greenstone belt in the northeastern Baltic Shield. *Earth-Science Reviews* 36, 205–241.
- Mikkola, P., 2008. Pre-Quaternary rocks of Northeast Kainuu. *Geological Survey of Finland, Report of Investigation* 175, 1–53 (in Finnish with English summary).
- Miller, C.F., Meschter McDowell, S. & Mapes, R.W., 2003. Hot and cold granites? Implications of zircon saturation temperatures and preservation of inheritance. *Geology* 31, 529–532.
- Papunen, H., Halkoaho, T. & Luukkonen, E., 2009. Archaean evolution of the Tipasjärvi-Kuhmo-Suomussalmi Greenstone Complex, Finland. *Geological Survey of Finland, Bulletin* 403, 1–68.
- Pearce, J.A., Harris, N.B.W. & Tindle, A.G., 1984. Trace element discrimination diagrams for the tectonic interpretation of granitic rocks. *Journal of Petrology* 25, 956–983.
- Rämö, O.T. & Luukkonen, E.J., 2001. 2.4 Ga A-type granites of the Kainuu region, eastern Finland: characterization

- and tectonic significance. In: EUG XI, April 8th - 12th, 2001, abstract volume.
- Rämö, O.T. & Haapala, I., 2005. Rapakivi granites. In: Lehtinen et al. (eds.) *Precambrian Geology of Finland: Key to the Evolution of the Fennoscandian Shield*. *Developments in Precambrian Geology* 14. Elsevier, Amsterdam, pp. 533–562.
- Rasilainen, K., Lahtinen, R. & Bornhorst, T.J., 2007. The Rock Geochemical Database of Finland Manual. Geological Survey of Finland, Report of Investigation 164, 1–38.
- Rosa D.R.N., Finch A.A., Andersen T. & Inverno C.M.C., 2009. U-Pb geochronology and Hf isotope ratios of magmatic zircons from the Iberian pyrite belt. *Mineralogy and Petrology* 95, 47–69.
- Schoene, B., Crowley, J.L., Condon, D.J., Schmitz, M.D. & Bowring, S.A., 2006. Reassessing the uranium decay constants for geochronology using ID-TIMS U–Pb data. *Geochimica et Cosmochimica Acta* 70, 426–445.
- Stacey, J.S. & Kramers, J.D., 1975. Approximation of terrestrial lead isotope evolution by a two-stage model. *Earth and Planetary Science Letters* 26, 207–221.
- Sun, S.S. & McDonough, W.F., 1989. Chemical and isotopic systematics of oceanic basalts: implications for mantle composition and processes. *Geological Society Special Publications* 42, 313–345.
- Vaasjoki, M., Taipale, K., Tuokko, I., 1999. Radiometric ages and other isotopic data bearing on the evolution of Archaean crust and ores in the Kuhmo-Suomussalmi area, eastern Finland. In: *Studies related to the Global Geoscience Transects/SVEKA Project in Finland*. *Bulletin of the Geological Society of Finland* 71, 155–176.
- Vuollo, J. & Huhma, H., 2005. Paleoproterozoic mafic dikes in NE Finland. In: Lehtinen et al. (eds.) *Precambrian Geology of Finland: Key to the Evolution of the Fennoscandian Shield*. *Developments in Precambrian Geology* 14. Elsevier, Amsterdam, pp. 195–236.
- Watkins, J.M., Clemens, J.D. & Treloar, P.J., 2007. Archaean TTGs as sources of younger granitic magmas: melting of sodic metatonalites at 0.6–1.2 GPa. *Contributions to Mineralogy and Petrology* 154, 91–110.
- Watson, E.B. & Harrison, T.M., 1983. Zircon saturation revisited: temperature and composition effects in a variety of crustal magma types. *Earth and Planetary Science Letters* 64, 295–304.
- Whalen, J.B., Currie, K.L. & Chappell, B.W., 1987. A-type granites: geochemical characteristics, discrimination and petrogenesis. *Contributions to Mineralogy and Petrology*, 95, 407–419.